Dalton Transactions

Cite this: *Dalton Trans.*, 2012, **41**, 11116

www.rsc.org/dalton

PAPER

Synthesis and evaluation of oxovanadium(IV) complexes of Schiff-base condensates from 5-substituted-2-hydroxybenzaldehyde and 2-substituted-benzenamine as selective inhibitors of protein tyrosine phosphatase 1B†

Hong Han,[a] Liping Lu,*[a] Qingming Wang,[a] Miaoli Zhu,*[a] Caixia Yuan,[a] Shu Xing*[b] and Xueqi Fu[b]

Received 27th January 2012, Accepted 9th July 2012
DOI: 10.1039/c2dt30198a

Five oxovanadium(IV) complexes, which were divided into two groups, $[V^{IV}O(bhbb, nhbb)(H_2O)_2]$ (tridentate ligands: H_2bhbb = 2-(5-bromo-2-hydroxylbenzylideneamino)benzoic acid, **1**; H_2nhbb = 2-(5-nitro-2-hydroxylbenzylideneamino)benzoic acid, **2**) and $[V^{IV}O(cpmp, bpmp, npmp)_2]$ (bidentate ligands: Hcpmp = 4-chloro-2-((phenylimino)methyl)phenol, **3**; Hbpmp = 4-bromo-2-((phenylimino)methyl)-phenol, **4**; Hnpmp = 4-nitro-2-((phenylimino)methyl) phenol, **5**) have been prepared and characterized by elemental analysis, infrared, UV-visible and electrospray ionization mass spectrometry. The coordination in $[V^{IV}O(bhbb)(H_2O)_2]$ (**1**) was confirmed by X-ray crystal structure analysis. The oxidation state of V(IV) with d^1 configuration in **1–5** was confirmed by EPR. The speciation of VO/H_2bhbb in methanol–aqueous solution was investigated by potentiometric pH titrations. The result indicated that the main species were $[V^{IV}O(bhbb)(OH)]^-$ and $[V^{IV}O(bhbb)(OH)_2]^{2-}$ at the pH range 7.0–7.4. The structure–activity relationship of the vanadium complexes in inhibiting protein tyrosine phosphatases (protein tyrosine phosphatase 1B, PTP1B; T-cell protein tyrosine phosphatase, TCPTP; megakaryocyte protein-tyrosine phosphatase, PTP-MEG2; Src homology phosphatase 1, SHP-1 and Src homology phosphatase 2, SHP-2) was investigated. The oxovanadium(IV) complexes were potent inhibitors of PTP1B, TCPTP, PTP-MEG2, SHP-1 and SHP-2, but exhibited different inhibitory abilities over different PTPs. Complexes **2** and **4** displayed better selectivity to PTP1B over the other four PTPs. Kinetic data showed that complex **2** inhibited PTP1B, TCPTP and SHP-1 with a noncompetitive inhibition mode, but a classical competitive inhibition mode for PTP-MEG2 and SHP-2. The results demonstrated that both the structures of vanadium complexes and the conformations of PTPs influenced PTP inhibition activity. The proper modification of the organic ligand moieties may result in screening potent and selective vanadium-based PTP1B inhibitors.

Introduction

Protein tyrosine phosphatases (PTPs) are a large family of signaling enzymes that play an important role in signal transduction and regulation of cellular processes.[1] Together with protein kinases, they control the level of phosphorylation of cells. Many human diseases, such as diabetes, obesity, cancer and immune disorders, are involved in the dysregulation of PTP activities.[2–6] As potential therapeutic targets, PTPs have attracted great attention in both academia and industry in past decades.[6–8]

PTP1B has been demonstrated to play key roles in the negative regulation of signaling pathways mediated by insulin receptors and leptin receptors. The PTP1B gene-null mice have increased insulin sensitivity and obesity resistance, even on a high-fat diet. Importantly, the PTP1B knockout mice are considered to be normal and do not show any other phenotypic characteristics.[9] PTP1B antisense oligonucleotide lowers PTP1B protein expression, normalizes blood glucose and improves insulin sensitivity in diabetic mice.[10] Some data suggest that PTP1B regulates insulin sensitivity in humans.[11–14] PTP1B has therefore emerged as a potential pharmaceutical target for the treatment of type II diabetes and obesity. Great efforts have been made in screening potent and selective PTP1B inhibitors in the last two decades. However, the common architecture of a PTP active site (*i.e.*, pTyr-binding pocket) impedes the development of selective PTP1B inhibitors. Therefore, it is a real challenge to design and exploit potent and specific PTP1B inhibitors.[15,16]

[a]*Institute of Molecular Science, Key Laboratory of Chemical Biology and Molecular Engineering of the Education Ministry, Shanxi University, Taiyuan, Shanxi 030006, P.R. China. E-mail: luliping@sxu.edu.cn, miaoli@sxu.edu.cn*
[b]*Edmond H. Fischer Signal Transduction Laboratory, College of Life Sciences, Jilin University, Changchun 130023, P.R. China. E-mail: xingshu@jlu.edu.cn*

†Electronic supplementary information (ESI) available. CCDC 862832 (**1**). Crystallographic data in CIF and BVS calculations for complex **1** and the experimental and simulation isotopic distribution patterns of ESI-MS spectra of complexes **1–5**. For ESI and crystallographic data in CIF or other electronic format see DOI: 10.1039/c2dt30198a

Vanadium is useful in the treatment of both type I and type II diabetes in various animal models, as well as in limited human trials.[17–22] Vanadium complexes with appropriate organic ligands can improve absorption, tissue uptake and potency, and decrease toxicity of the metal. Organic vanadium complexes exhibit high insulin-mimetic potential with low side effects compared to inorganic vanadium. A bis(maltolato)oxovanadium(IV) (BMOV) derivative was tested on phase II clinical trials as an antidiabetic drug.[22] The inhibition of PTPs that dephosphorylate the insulin receptor, resulting in prolongation of insulin signaling, is involved in the mechanism of vanadium's insulin-sensitizing effects.[23,24] *In vitro* experiments have demonstrated that vanadium complexes can inhibit PTP1B. Pervanadate inhibits PTP1B by irreversibly oxidizing the catalytic cysteine to a SO_3H group, while vanadate and vanadium complexes competitively inhibit PTP1B.[24–32] However, few studies have investigated the inhibition against other PTPs and the selectivity of vanadium complexes. It is worth mentioning that the latest research shows metal-based PTP selective inhibitors exhibit consistent selectivity in cells as for *in vitro* results,[33,34] suggesting that *in vitro* screened metal-based selective PTP inhibitors may work *in vivo*. Thus, it is promising to carry out a wide investigation into screening PTP1B selective inhibitors among vanadium complexes in order to improve the potency of vanadium-based antidiabetic drugs and decrease their side effects. As a matter of fact, our recent study revealed that several vanadium complexes do display some selectivity against PTP1B,[28,30] inspiring us to screen potent and selective vanadium-based PTP1B inhibitors by modifying the ligands of vanadium complexes.

In this report, a series of oxovanadium complexes of Schiff bases have been synthesized and well characterized. Their inhibitory effects against five PTPs are evaluated. The results show these complexes are potent PTPs inhibitors and have certain selectivity against PTP1B.

Experimental section

Materials and methods

All reagents and solvents were obtained from commercial sources and used without further purification unless specially noted. Double distilled water was used to prepare buffer solutions.

Physical measurement

The C, H and N analyses were performed on a VARI-EL elemental analyzer. IR spectra on KBr pellets were recorded on a Shimadzu FT IR-8300 spectrometer in the range of 4000–400 cm^{-1} (KBr disks). The electronic spectra were recorded on a Hewlett-Packard HP-8453 Chemstation spectrophotometer. UV-Vis spectra of titrations of ligands (2 ml, 5×10^{-5} M) with $VOSO_4$ (2.5×10^{-3} M) were used in the study in DMSO–aqueous solution (1 : 9) at room temperature. Electrospray ionization mass spectra (ESI-MS) were recorded with a micrOTOF-Q instrument (Bruker) in methanol solution. The EPR spectrum was obtained in solid and DMSO solution at 110 K on a Bruker-ER 200-D-SRC spectrometer. The EPR spectrum of a frozen sample was simulated by use of the WinEPR SimFonia program developed and supported by Bruker Company. The X-ray data were collected on a Bruker SMART APEX 1K CCD diffractometer. Bioactivity assays (IC_{50} values) of the complexes were carried out on SpectraMax M5 Multi-Mode Microplate Readers (Molecular Devices, USA), as previously described.[28–31]

Synthesis of the complexes

The synthesis of Schiff bases and oxovanadium(IV) complexes **1–5** followed the routes described in Scheme 1. Tridentate and bidentate Schiff base ligands were synthesized from an equimolar mixture of 5-X-salicylaldehyde (X = Cl, Br and NO_2) with anthranilic acid or aniline by use of the respective procedures previously reported.[35] Next, the object complexes were synthesized by the Schiff bases reacted with $VOSO_4{\cdot}xH_2O$ in methanol solution.

2-((5-Bromo-2-oxybenzylidene)amino)benzoato-diaqua-oxovanadium(IV) (1). 0.14 g (1.0 mmol) anthranilic acid and 0.16 g (2.0 mmol) NaOAc were thoroughly dissolved in 10 mL of water with a constant stirring. To it 0.20 g (1.0 mmol) 5-bromo-salicylaldehyde in 10 mL of absolute ethanol was added dropwise. After several minutes, 0.23 g (1.0 mmol) of $VOSO_4{\cdot}xH_2O$ in 3.0 mL of water was added dropwise. The reaction mixture was heated under refluxing for 3 h. After cooling slowly, the brown precipitates were separated out. The separated compound was filtered, washed thoroughly with absolute ethanol and water, and then dried in a vacuum desiccator with P_2O_5. Yield 41%, element analysis (EA) for **1**($C_{14}H_{12}BrNO_6V$), calcd/found(%): C 39.93/39.75, H 2.87/3.14, N 3.33/3.28; IR (s = strong, m = medium, w = weak): $\nu_{C=N}$ 1577s (1604s in H_2bhbb), $\nu_{V=O}$ 982m (995 cm^{-1} in $VOSO_4$); ESI-MS(*m*/*z*, a negative mode, see Table 1 and ESI†), observed molecular ion peak (*I*%): 420.86(38%) for $[\mathbf{1} - H]^-$ 420.92; UV-Vis(DMSO): λ_{max}/nm ($\varepsilon \times 10^4/M^{-1}\ cm^{-1}$), 264(2.37), 290–310(1.45), 412(0.85).

A brown crystal of **1** was obtained by slow evaporation of the reaction solution at room temperature after two weeks.

2-((5-Nitro-2-oxybenzylidene)amino)benzoato-diaqua-oxovanadium(IV) (2). Following the same procedures as described in synthesis of **1**, received **2** with 5-nitro-salicylaldehyde instead of 5-bromo-salicylaldehyde. Yield 30%, EA for **2** ($C_{14}H_{12}N_2O_8V$), calcd/found(%): C 43.43/43.85, H 3.12/3.01, N 7.23/7.34; IR: $\nu_{C=N}$ 1562s (1611s in H_2nhbb), $\nu_{V=O}$ 952m; ESI-MS(*m*/*z*, a negative mode, see Table 1 and ESI†), observed molecular ion peak (*I*%): 385.94(38%) for $[\mathbf{2} - H]^-$ 386.00; UV-Vis(DMSO): λ_{max}/nm ($\varepsilon \times 10^4/M^{-1}\ cm^{-1}$), 262(1.26), 307(1.38), 376(1.79).

Bis(4-chloro-2-((phenylimino)methyl)phenolate)-oxovanadium(IV) (3). Hcpmp was precipitated by the condensation of 5-chloro-salicylaldehyde and aniline in absolute ethanol. 3.13 g (20.0 mmol) 5-chloro-salicylaldehyde was dissolved in 30 mL of absolute ethanol. To this, 1.8 mL (20.0 mmol) of aniline was added dropwise with a constant stirring. The reaction mixture was heated under refluxing for 3 h. After cooling slowly, the light orange needle crystals were separated out. The separated compound was filtered, washed thoroughly with absolute ethanol and dried in a vacuum desiccator with P_2O_5. Yield 82%, EA for Hcpmp($C_{13}H_{10}ClNO$), calcd/found(%): C 67.39/67.54, H 4.35/4.35, N 6.05/5.82; IR: $\nu_{C=N}$ 1614s. A 0.46 g sample (2.0 mmol)

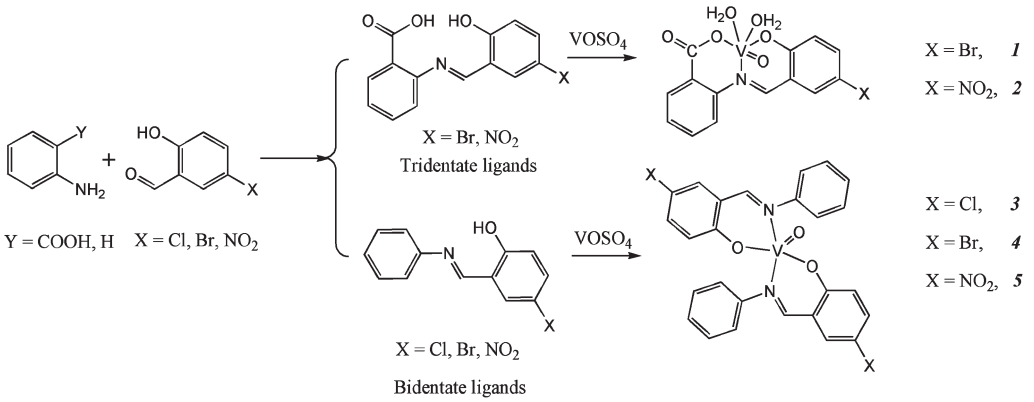

Scheme 1 Schematic routes of the synthesis of the complexes **1**–**5**, [$V^{IV}O$(bhbb)](**1**), [$V^{IV}O$(nhbb)](**2**), [$V^{IV}O(cpmp)_2$](**3**), [$V^{IV}O(bpmp)_2$](**4**), [$V^{IV}O(npmp)_2$] (**5**).

of the ligand in 15.0 mL of absolute ethanol was heated under refluxing until thoroughly dissolved and 0.45 g (2.0 mmol) of $VOSO_4$ in 10.0 mL of water was added dropwise with constant stirring. The reaction mixture was adjusted to pH = 7 with NaOH solution and then it was heated under refluxing for 4 h. After cooling slowly, the green precipitates were separated out. The separated compound was filtered, washed thoroughly with absolute ethanol and water, and then dried in a vacuum desiccator with P_2O_5. Yield 84%, EA for **3**($C_{26}H_{18}Cl_2N_2O_3V$), calcd/found(%): C 59.11/59.20, H 3.43/3.47, N 5.30/5.19; IR: $\nu_{C=N}$ 1559s, $\nu_{V=O}$ 973m; ESI-MS(*m*/*z*, a positive mode, see Table 1 and ESI†), observed molecular ion peak (*I*%): 528.04(94%) for $[\mathbf{3} + H]^+$ 528.02; UV-Vis(DMSO): λ_{max}/nm ($\varepsilon \times 10^4/M^{-1}\ cm^{-1}$), 262(1.78), 344(1.33).

Bis(4-bromo-2-((phenylimino)methyl)phenolate)-oxovanadium(IV) (4). Following the same procedures as described in synthesis of Hcpmp, received Hbpmp with 5-bromo-salicylaldehyde instead of 5-chloro-salicylaldehyde. Hbpmp yield 91%, EA for Hbpmp($C_{13}H_{10}BrNO$), calcd/found(%): C 56.55/56.58, H 3.65/3.69, N 5.07/5.11; IR: $\nu_{C=N}$ 1614s. 0.46 g (2.0 mmol) of Hbpmp in 10.0 mL of absolute ethanol was thoroughly dissolved with constant stirring, 0.16 g (2.0 mmol) NaOAc was added to the solution, and then 0.23 g (1.0 mmol) of $VOSO_4 \cdot xH_2O$ in 3.0 mL of water was added dropwise with constant stirring. The reaction mixture was refluxed for 3 h. After cooling slowly, the green precipitates **4** were separated out. The separated compound was filtered, washed thoroughly with absolute ethanol and water, and then dried in a vacuum desiccator with P_2O_5. Yield 70%, EA for **4**($C_{26}H_{18}Br_2N_2O_3V$), calcd/found(%): C 50.60/50.60, H 2.94/2.98, N 4.54/4.48; IR: $\nu_{C=N}$ 1559s, $\nu_{V=O}$ 982m; ESI-MS (*m*/*z*, a positive mode, see Table 1 and ESI†), observed molecular ion peak (*I*%): 616.92(48%) for $[\mathbf{4}]^+$ 617.18; UV-Vis (DMSO): λ_{max}/nm ($\varepsilon \times 10^4/M^{-1}\ cm^{-1}$), 263(1.88), 344(1.43).

Bis(4-nitro-2-((phenylimino)methyl)phenolate)-oxovanadium(IV) (5). Following the same procedures as described in synthesis of **3**, received Hnpmp and **5** with 5-nitro-salicylaldehyde instead of 5-chloro-salicylaldehyde. Hnpmp yield 91%, EA for Hnpmp($C_{13}H_{10}N_2O_3$), calcd/found(%): C 64.46/64.45, H 4.16/4.10, N 11.56/11.14; IR: $\nu_{C=N}$ 1620s. **5** yield 30%, EA for **5**($C_{26}H_{18}N_4O_7V$), calcd/found(%): C 56.84/56.60, H 3.30/3.36, N 10.20/9.95; IR: $\nu_{C=N}$ 1560s, $\nu_{V=O}$ 947m; ESI-MS(*m*/*z*, a positive mode, see Table 1 and ESI†), observed molecular ion peak (*I*%): 549.07(100%) for $[\mathbf{5}]^+$ 549.06; UV-Vis(DMSO): λ_{max}/nm ($\varepsilon \times 10^4/M^{-1}\ cm^{-1}$), 261(1.95), 298(1.65), 364(2.97), 429(1.48).

X-ray crystallography

A single crystal of the complex **1**·1.5H_2O was mounted on glass fibers for data collection. Cell parameters and an orientation matrix for data collection were obtained by least-square refinement of diffraction data from 6213 reflections with 2.41–25.26° of θ for **1**·1.5H_2O using a Bruker SMART APEX 1K CCD automatic diffractometer. Data were collected at 298 K using MoKα radiation (λ = 0.71073 Å) and the ω-scan technique, and corrected for Lorentz and polarization effects (SADABS).[36] The structures were solved by direct methods (SHELXS-97)[37] and subsequent difference Fourier maps and then refined on F^2 by a full-matrix least-squares procedure using anisotropic displacement parameters.[37] After several cycles of refinement, hydrogen atoms attached to C atoms were located at their calculated positions with C(sp^2)–H 0.93 and were refined using a riding model. H atoms attached to O atoms in **1**·1.5H_2O were located from difference Fourier maps and their global U_{iso} value refined. Molecular graphics are from Ortep3.[38]

Potentiometric titration

pH-Potentiometric titration was performed to study the species formed in solution. The experiment was carried out in 20% methanol–water (by volume) due to the poor solubility of H_2bhbb and its complexes in pure water. The ionic strength of the solutions was maintained by 0.2 M NaCl. The protonation constants of ligands and the stability constants of the complexes $VOSO_4$ with ligands were determined by pH-potentiometric titrations of 40 mL samples containing the ligand being acidified by HCl. High-purity nitrogen gas was used to remove carbon dioxide and molecular oxygen from samples and to provide an inert gas atmosphere during all measurements. Measurements of the pH values were carried out at 298 ± 0.2 K on a PHS-3TC pH meter with a combined glass electrode. The electrode was

Table 1 Characteristics of complexes[a]

Complex, yield (%)	IR (cm^{-1}) $\nu_{C=N}$,$\nu_{V=O}$[b]	EPR[c] (g)	UV-Vis DMSO,λ_{max}/nm ($\varepsilon \times 10^4/M^{-1}\ cm^{-1}$)	ESI-MS[d](m/z) isotopic peaks Species calcd/found
1, 41%	1577s, 982s	1.981	264(2.37), 290–310(1.45), 412(0.85)	$[\mathbf{1}-H]^-$ 417.92–423.93/417.90–423.86
2, 30%	1562s, 952s	1.976	262(1.26), 307(1.379), 376(1.786)	$[\mathbf{2}-H]^-$ 385.00–389.00/385.56–388.92
3, 84%	1559s, 973s	2.011	262(1.78), 344(1.33)	$[\mathbf{3}+H]^+$ 526.02–533.01/526.02–533.02
4, 70%	1559s, 982s	2.023	263(1.88), 344(1.43)	$[\mathbf{4}+H]^+$ 613.62–622.32/613.92–621.92
5, 30%	1560s, 947s	1.975	261(1.95), 298(1.65), 364(2.97), 429(1.48)	$[\mathbf{5}+H]^+$ 547.98–552.07/548.06–552.07

[a] Element analysis: see experimental section. [b] 995 cm^{-1} in $VOSO_4$, s for strong. [c] In solid at 110 K. [d] In methanol.

calibrated by standard buffer solutions. The titrations were performed with a carbonate-free NaOH solution of known concentration (0.09495 M) using a microsyringe under a nitrogen atmosphere in a jacketed vessel. The protonation constants of ligands and the equilibrium constants of the complexes were calculated with the aid of the SUPERQUAD program.[39] The correction ionization constants of water in 20% methanol–water mixtures were taken from Wooley *et al.*,[40] namely $pK_{M/W} = [H^+][A^-] = 14.10$, where A^- is OH^- and CH_3O^-. The overall formation constant of the complex is denoted as the logarithm of $\beta_{pqr} = [VO_pH_2bhbb_qH_r]/[VO]^p[H_2bhbb]^q[H]^r$. The conventional notation has been used: negative indices for H in the formulas indicate the dissociation of groups that do not deprotonate in the absence of either V(IV)O coordination or hydroxo ligands. The following hydroxo species of VO^{2+} were taken into account in the calculations: $[VO(OH)]^+$ (log $\beta_{10\text{-}1} = -5.94$) and $[(VO)_2(OH)_2]^{2+}$ (log $\beta_{20\text{-}2} = -6.95$),[41] $[VO(OH)_3]^-$ (log $\beta_{10\text{-}3} = -18.0$) and $[(VO)_2(OH)_5]^-$ (log $\beta_{20\text{-}5} = -22.0$).[42] All solutions were freshly prepared before use. As in our previous report,[30] the cumulative stability constants (β_{pqr}) of oxovanadium complex species in the V(IV)O/H_2bhbb system were log $\beta_{111} = 14.97(4)$, log $\beta_{110} = 9.44(9)$, log $\beta_{11\text{-}1} = 4.94(4)$, log $\beta_{11\text{-}2} = -2.91(4)$ and log $\beta_{11\text{-}3} = -13.15(5)$.

Protein tyrosine phosphatase inhibition assays

Human PTPs were expressed and purified as described previously.[43–46] PTP activities were measured using *p*-nitrophenol phosphate (*p*NPP) as the substrate. The assays were performed in 20 mM 3-morpholinopropanesulfonic acid (MOPS) buffer, pH 7.2, containing 50 mM NaCl and 2 mM GSH (L-glutathione(reduced)). Complexes **1–5** were dissolved in DMSO (10^{-2} M) and diluted to various concentration gradients, and further diluted 10 times into enzyme-MOPS buffer solutions for activity evaluations. Inhibition assays were performed in the same buffer on a 96-well plate in 100 μL volumes. Namely, 10 μL of complex with various concentrations was mixed to 82 μL enzyme solution for 30 min. Then 2 μL of *p*NPP (0.1 M) substrate was added to initiate enzyme reactions. After incubation for 30 min at room temperature, the reactions were terminated by the addition of 6 μL of 2 M NaOH. The optical density at 405 nm was measured on a microplate reader. IC_{50} values were obtained by fitting the concentration-dependent inhibition curves by use of the Origin program. All data points were carried out in triplicate. Solutions of the oxovanadium complexes were all freshly prepared before each experiment.

The inhibiting kinetic analysis was performed according to eqns (1) and (2) for competitive and noncompetitive inhibition modes, respectively, where V_{max} is the maximum initial velocity, K_m for the corresponding Michaelis–Menten constant, S for the substrate, I for the inhibitor and K_i for the inhibition constant at varied substrate concentrations, derived from the slope of the Lineweaver–Burk plots.

$$\frac{1}{v} = \frac{K_m}{V_{max}}\left(1 + \frac{[I]}{K_i}\right)\frac{1}{S} + \frac{1}{V_{max}} \quad (1)$$

$$\frac{1}{v} = \frac{K_m}{V_{max}}\left(1 + \frac{[I]}{K_i}\right)\frac{1}{S} + \frac{1}{V_{max}}\left(1 + \frac{[I]}{K_i}\right) \quad (2)$$

Inhibition constants were determined by the measurement of initial hydrolysis rates at different concentrations of substrate and inhibitor. The apparent Michaelis–Menten constant (K_{app}) values measured at the various inhibitor concentrations were plotted against concentration of the inhibitor to calculate the K_i values. For the K_i value of each PTP, the measurements were independently repeated at least three times.

Results and discussion

Synthesis and general aspects

The oxovanadium complexes were prepared from a typical synthetic procedure, in which oxovandium(IV) sulfate is reacted *in situ* with dianionic or monoanionic Schiff bases in methanol–aqueous solution, as shown in Scheme 1, in which the intermediate tridentate Schiff bases are not isolated. All of the vanadium complexes are elucidated on the basis of the EAs, IR, EPR, UV-Vis and ESI-MS. Selected characteristics of the complexes are listed in Table 1. The complexes are remarkably soluble in DMSO, soluble in methanol and insoluble in water. The elemental analysis data for **1–5** are consistent with the compositions of the desired products. They are confirmed by an ESI-MS study (see Table 1 and ESI†). Complex **1** is further supported by X-ray single crystal diffraction in the forthcoming discussion. In the infrared spectra, the absorption bands at *ca.* 1559–1577 cm^{-1} can be assigned to the C=N vibration involving coordination through the nitrogen of the azomethine group. The V=O stretching frequencies of the complexes occur in the range of 947–982 cm^{-1}, which is consistent with the previously reported range observed for the majority of oxovanadium(IV) complexes.[28–31] The electronic absorption spectra of the oxovanadium(IV) complexes in DMSO show a progress of ligand-to-

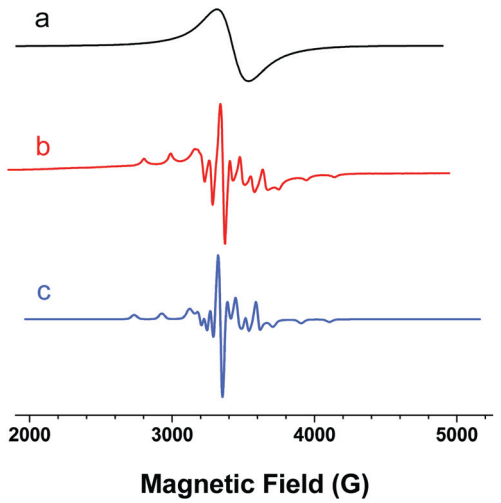

Fig. 1 EPR spectra of complex **1**, (a) powder sample at 110 K, (b) frozen sample in DMSO at 110 K and (c) the simulated spectrum of frozen sample.

metal charge transfer (LMCT) from occupied π(n) orbitals of the chelated ligand to empty d orbitals of the vanadium near 344–429 nm (Table 1).

In order to ascertain the oxidation state of the vanadium, electron paramagnetic resonance was employed. As shown in Fig. 1, the X-band EPR spectra of complex **1** of the solid powder and frozen sample in DMSO at 110 K, which exhibits an axially symmetrical signal of tetravalent vanadium in solution, split into a number of hyperfine lines which originate from the d^1 electron interaction with a nuclear spin $I = 7/2$. The spectrum displays well-resolved ^{51}V ($I = 7/2$) hyperfine lines. Furthermore, bond valence sum (BVS) calculations show a value of 4.14 for the V center. This value is clearly within the stipulated error limit.[47] Thus, an oxidation state of +4 is assigned to vanadium (see ESI†). This agrees with the result of EPR analysis.

Molecular structure of complex 1

Complex **1**·1.5H_2O crystallizes in space groups $C_{2/c}$. Some parameters on the crystal data and structure determination are summarized in Table 2. Coordination parameters of vanadium are shown in Table 3 and the structure is shown in Fig. 2.

The structure of the complex consists of a monomeric oxovanadium(IV) species with a VO^{2+} moiety bonded by two chelate rings of one dianionic tridentate Schiff base, namely, V1/O2/C2/C1/C7/N1 and V1/N1/C8/C13/C14/O3. The complex has a $V^{IV}O_5N$ distorted octahedron geometry with a V═O distance of 1.585(2) Å, typical for a double bond. The Schiff base is bound through the phenolate oxygen (O2), the imine nitrogen (N1) and the carboxylate oxygen (O3) of the ligand, which cooperate with O5 atom of water to form the equatorial plane and O1 bond to V1 and O6 (water) atoms located at the axial positions. Due to the Jahn–Teller effect in a d^1 electron configuration of vanadium(IV), the V1–O6 bond trans to the V═O group is significantly longer (2.248(2) Å) than the other two V–O bonds (Table 3). The V–O distances involving the Schiff bases and water are in range of 1.957(2)–2.056(2) Å in **1**, typical for single bonds. The lattice water molecules in the complex **1** show intermolecular H-bonding interactions with coordinated water and the carboxylate oxygen of the Schiff base (Fig. 2 and Table 4).

Table 2 Crystallographic data of complex **1**

	1·1.5H_2O
CCDC number	862832
Formula	$C_{14}H_{12}BrNO_6V·1.5H_2O$
Formula weight	448.12
Wavelength (Å)	0.71073(Mo Kα)
Temperature (K)	298(2)
Crystal system	monoclinic
Space group	*C*2/*c*
a (Å)	33.835(4)
b (Å)	7.374(1)
c (Å)	13.086(2)
β (°)	92.497(2)
V (Å^3)	3261.8(7)
Crystal size (mm)	0.20 × 0.15 × 0.10
Z	8
D_{calc} (g cm^{-3})	1.825
μ (mm^{-1})	3.099
F_{000}	1792
θ range (°)	1.2–25.59
Limiting indices, *h*	$-40 \le h \le 40$
K	$-8 \le k \le 8$
L	$-15 \le l \le 15$
Goodness-of-fit	1.029
Reflections collected	17390
Reflections unique	3051
R_{int}	0.0354
Final *R* [$I > 2\sigma(I)$]	0.0245
R (all data)	0.0320
Completeness	0.998
Largest diff. peak and hole (e Å^3).	0.298, −0.354

Table 3 Coordinated geometry of complex **1**

Bond length, Å		Bond angle, °			
V1–O1	1.585(2)	O1–V1–O2	101.6(1)	O2–V1–N1	91.6(1)
V1–O2	1.957(2)	O1–V1–O3	102.7(1)	O3–V1–N1	88.1(1)
V1–O3	1.985(2)	O2–V1–O3	155.6(1)	O5–V1–N1	169.8(1)
V1–O5	2.056(2)	O1–V1–O5	93.9(1)	O1–V1–O6	179.4(1)
V1–N1	2.078(2)	O2–V1–O5	87.3(1)	O2–V1–O6	78.5(1)
V1–O6	2.248(2)	O3–V1–O5	88.7(1)	O3–V1–O6	77.2(1)
N1–C7	1.295(3)	O1–V1–N1	96.3(1)	O5–V1–O6	85.5(1)
		N1–V1–O6	84.3(1)	C7–N1–C8	117.7(2)

Chemistry in solution

The interaction of the ligands with the oxovanadium(IV) was analyzed by use of UV-Vis titration experiments in order to explore the structure of the complex in aqueous solution. Here, we take H_2nhbb and Hnpmp as representatives of tridentate and bidentate ligands. UV-Vis titration of complexes **2** and **5** were performed in aqueous solution including 10% DMSO. As shown in Fig. 3, ligands H_2nhbb and Hnpmp and $V^{IV}O$ ion easily form the complexes [VO(nhbb)] (1 : 1) and [VO(npmp)$_2$] (2 : 1), respectively, in which the ratio of tridentate and bidentate Schiff bases binding to $V^{IV}O$ is 1 : 1 and 2 : 1. The results agree with those in the solid structure studies of complexes **2** and **5**.

The five complexes were further characterized by ESI-MS in methanol solution. As shown in Table 1 and ESI,† species corresponding to the molecular ion are observed for all of the

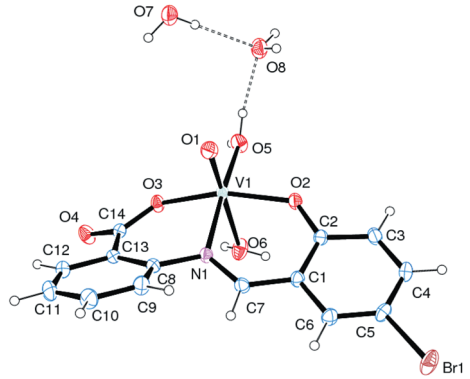

Fig. 2 An ORTEP view of complex **1** showing atom labeling with 30% probability thermal ellipsoids, double dash lines for H-bonds.

Table 4 Hydrogen bonds in **1** (Å, °)[a]

D–H···A	*d*(D–H)	*d*(H···A)	*d*(D···A)	∠(DHA)
O5–H5···O8	0.86(4)	1.86(4)	2.714(3)	173(4)
O5–H5B···O3^{i}	0.83(4)	1.88(4)	2.671(2)	156(3)
O6–H6···O7^{ii}	0.75(3)	2.00(4)	2.743(3)	169(3)
O6–H6B···O4^{iii}	0.75(3)	2.10(4)	2.839(3)	172(4)
O7–H7A···O8	0.83(3)	1.91(3)	2.721(3)	166(3)
O8–H8A···O4^{iv}	0.79(4)	2.17(4)	2.950(3)	169(3)
O8–H8B···O2^{v}	0.95(5)	1.95(5)	2.897(3)	177(4)
C3–H3···O1^{vi}	0.93	2.41	3.116(3)	133

[a] Symmetry codes: (i) $-x+1, y, -z+1/2$; (ii) $x, y-1, z$; (iii) $x, -y, z+1/2$; (iv) $x, -y+1, z+1/2$; (v) $-x+1, -y+1, -z+1$; (vi) $x, 1-y, 1/2+z$.

complexes. The compositions of the complexes deduced from the elemental analysis are confirmed by the ESI-MS study and the corresponding parent peaks in the ESI-MS exclude immediate hydrolysis of the complexes in methanol solution.[48]

In addition, the data of the potentiometric titration of the system of $V^{IV}O$ cation and H_2bhbb shows the species distribution of the complexes formed in aqueous solution, which is relevant to their bioactivities. On the basis of these data, the species distribution diagram as a function of pH is shown in Fig. 4. The distribution curves suggest that the oxovanadium species $[VO(bhbb)(OH)]^{-}$ and $[VO(bhbb)(OH)_2]^{2-}$ are predominant in the pH range 7.0–7.4.

Recombinant PTPs inhibition assays

The five complexes were tested for their abilities in inhibiting PTP1B, TCPTP, PTP-MEG2, SHP-1 and SHP-2 by use of *p*NPP as the substrate. The IC_{50} values are listed in Table 5. The results show that almost all of the five complexes display strong inhibition against PTP1B, though their inhibitory abilities vary over different PTPs. Complexes **1** and **2** with a ligand:V ratio of 1 : 1 have slightly stronger inhibitory effects against PTP1B (IC_{50}, 0.21–0.23 μM) than **3–5** possessing a ligand:V ratio of 2 : 1 (IC_{50}, 0.69–0.93 μM). The potency of PTP1B inhibitions of the five complexes are obviously weaker than that of our previously reported ternary oxovanadium(IV) complexes of ONO-donor Schiff bases and polypyridyl derivatives, but equivalent to

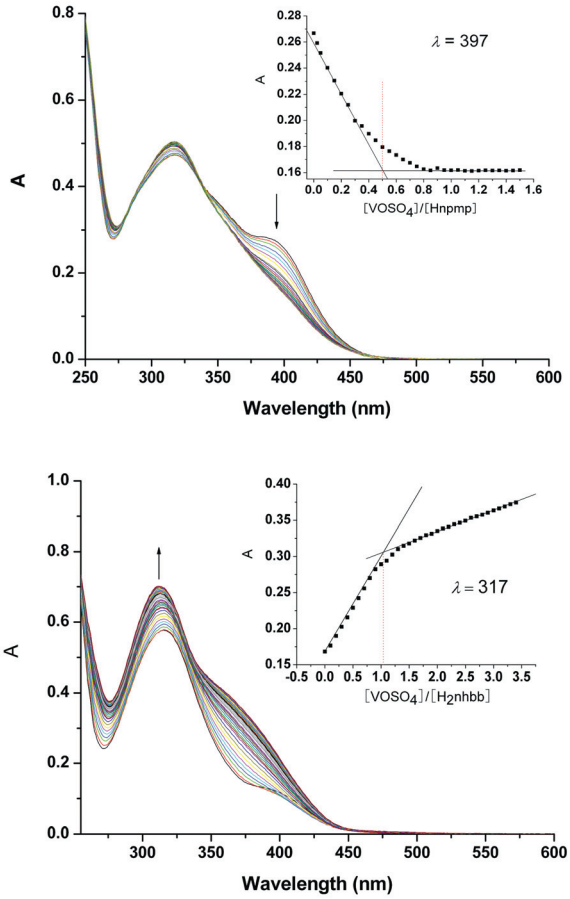

Fig. 3 UV-Vis spectra of titrations of Hnpmp (up) and H_2nhbb (bottom) (2 mL, 5×10^{-5} M) with $VOSO_4$ (5×10^{-3} M) used in the study in DMSO–aqueous solution (1 : 9) at room temperature.

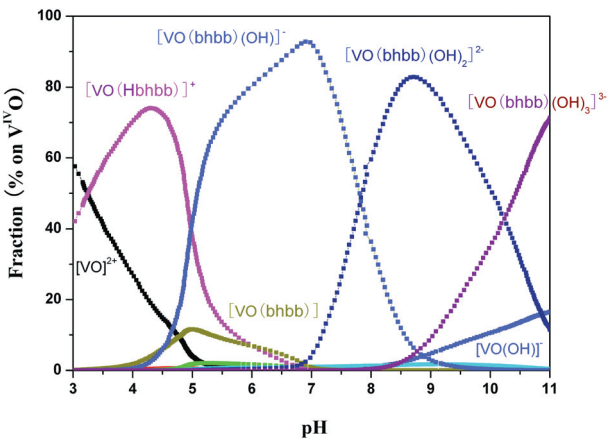

Fig. 4 Species distribution as a function of pH for VO-H_2bhbb (1 : 1, 0.75 mM) systems.[30] Coordinated water molecules were omitted.

$Na_2[VO(Glu)_2(CH_3OH)]$ and the most ternary oxovanadium(IV) complexes of amino-acid Schiff bases and polypyridyl derivatives, as well as BMOV (Table 5). In both 1 : 1 complexes, **2** shows better selectivity against PTP1B over the other four PTPs. The inhibitory ability against PTP1B is about 5, 3, 8 and 20-fold stronger than that against TCPTP, PTP-MEG2, SHP-1 and

Table 5 IC_{50}(S.D.)(μM)[a] of oxovanadium complexes on five PTPs

	PTP1B	TCPTP	PTP-MEG2	SHP-1	SHP-2	Ref.[b]
1	0.21(2)	0.19(3)	0.97(6)	3.0(3)	49(9)	R1
2	0.23(1)	1.3(1)	0.60(9)	1.9(2)	4.2(4)	R1
3	0.80(9)	8.3(7)	3.6(4)	1.0(2)	2.3(6)	R1
4	0.69(3)	1.9(3)	2.9(4)	6.5(3)	35(3)	R1
5	0.93(9)	1.4(1)	3.2(6)	2.5(5)	2.6(2)	R1
S1[c]	0.030	0.054		0.26		30
S2[d]	0.86(2)					49
S3[e]	0.29	0.34		0.21		31

[a] All data points were carried out in triplicates. [b] R1 for this work. [c] **S1** = [VO(SAA)(bpy)]. [d] **S2** = BMOV. [e] **S3** = $Na_2[VO(Glu)_2(CH_3OH)]$.

SHP-2, while complex **1** displays a similar inhibitory effect over PTP1B and TCPTP, but about 5, 15 and 250-fold stronger than over PTP-MEG2, SHP-1 and SHP-2. In the three 2 : 1 complexes, complex **4** seems to be more selective in inhibiting PTP1B. The potency against PTP1B is more efficient by about 3, 4, 10 and 50-fold than against TCPTP, PTP-MEG2, SHP-1 and SHP-2. Complex **3** exhibits comparable inhibitory ability against PTP1B and SHP-1, and about 10, 3 and 2-fold stronger inhibition against TCPTP, PTP-MEG2 and SHP-2, while complex **5** shows lower selectivity with comparable inhibition against PTP1B and TCPTP, and about only 2 to 3-fold stronger against the other three. Our previous study shows that ternary oxovanadium(IV) complexes of ONO-donor Schiff bases and

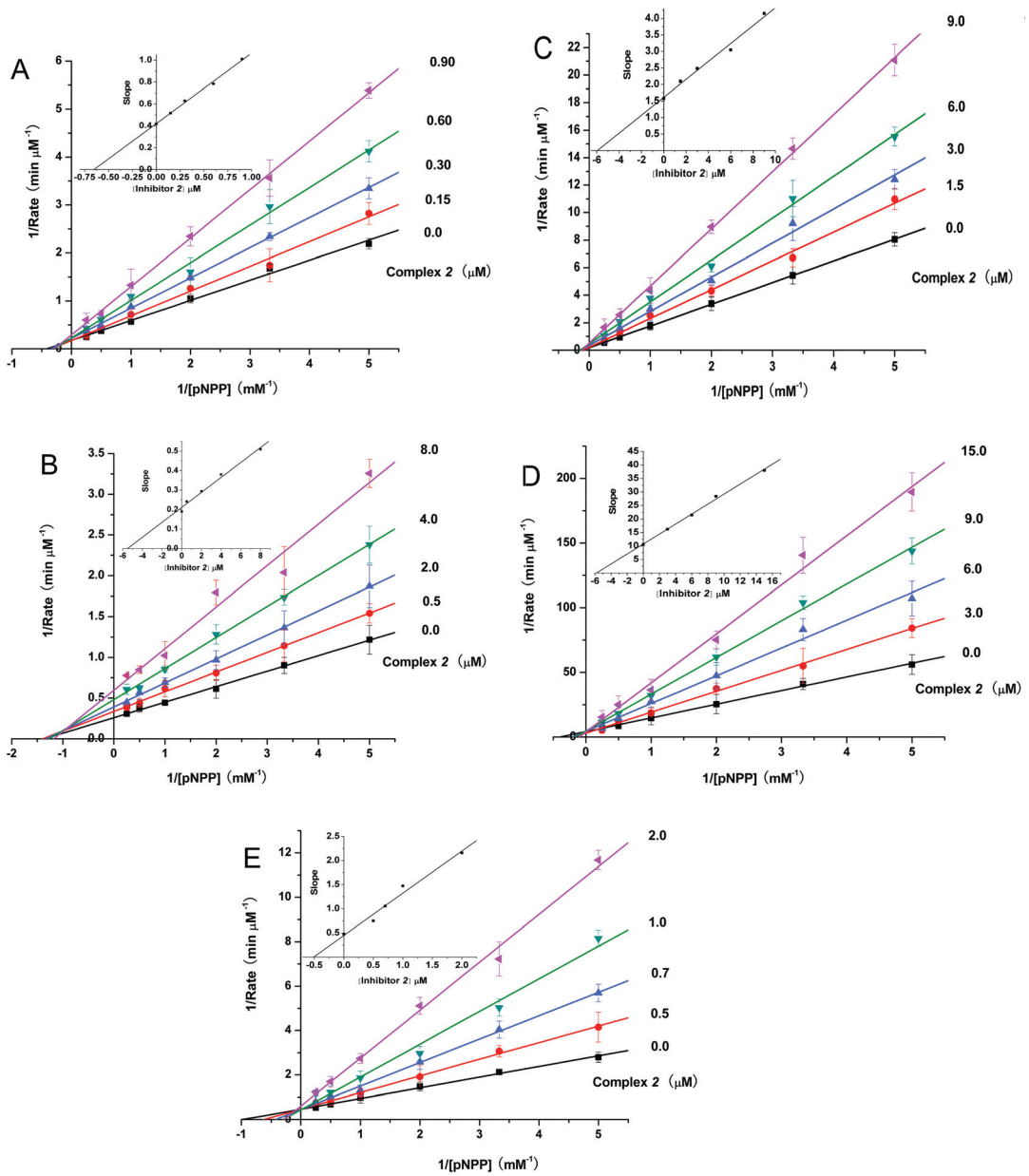

Fig. 5 Lineweaver–Burk plots of $1/v$ (min mM^{-1}) *vs.* the reciprocal of the *p*NPP concentrations (mM^{-1}) at five fixed concentrations of complex **2** for PTP1B (A), TCPTP (B), SHP-1 (C), SHP-2 (D) and PTP-MEG2 (E), error bars represent ±S.D. Inset: determination of K_i for complex **2** inhibiting PTP1B, TCPTP, SHP-1, SHP-2 and PTP-MEG2, respectively.

polypyridyl derivatives selectively inhibit PTP1B 2-fold and 10-fold stronger than TCPTP and SHP-1, but $Na_2[VO(Glu)_2(CH_3OH)]$ almost equally inhibit PTP1B, TCPTP, SHP-1 and HePTP (hematopoietic tyrosine phosphatase). Obviously, complexes **2** and **4** show better selectivity to PTP1B. All of these results illustrate that the ligands of vanadium complexes influence the inhibitory effects of different PTPs. Properly modifying the organic ligand moieties on vanadium may result in screening potent and selective vanadium-based PTP1B inhibitors.

Kinetic analysis of recombinant PTPs inhibition

Complex **2** was further chosen to investigate the inhibition mode of the five PTPs because of its stronger potency and better selectivity against PTP1B. As shown in Fig. 5, for PTP1B, TCPTP and SHP-1, the Lineweaver–Burk double-reciprocal plot of the kinetic data of complex **2** shows that the lines converge at an intersection on the *x*-axis left of the *y*-axis, implying a noncompetitive inhibition mode *versus* *p*NPP, while the lines converge at an intersection on the *y*-axis above the *x*-axis for PTP-MEG2 and SHP-2, indicating a classical competitive inhibition mode *versus* *p*NPP. The inhibition constants (K_i) for PTP1B, TCPTP, SHP-1, PTP-MEG2 and SHP-2 are calculated to be 0.65, 5.5, 6.0, 0.51 and 5.8 μM, respectively (Fig. 5, inset). The different inhibition modes over the five PTPs demonstrate that with the variation of PTPs conformations, vanadium complexes bind different PTPs at different sites. Compared with previous reports that vanadium complexes inhibit PTP1B in a competitive inhibition mode,[24,26,28–31] the noncompetitive inhibition mode of complex **2** inhibiting PTP1B suggests that as the structure changes, vanadium complexes can bind to PTP1B at different sites. The results illustrate that both the structures of vanadium complexes and the conformations of PTPs influence the PTPs inhibition, which provide a greater opportunity to screen potent and selective PTP1B inhibitors.

Conclusions

In summary, we have synthesized and characterized five oxovanadium(IV) complexes. Biochemical assays demonstrate that the oxovanadium(IV) complexes are potent inhibitors of PTP1B, TCPTP, PTP-MEG2, SHP-1 and SHP-2, but exhibit different inhibitory abilities over different PTPs. Complexes **2** and **4** display better selectivity to PTP1B over the other four PTPs. Kinetic data show complex **2** inhibits PTP1B, TCPTP and SHP-1 with a noncompetitive inhibition mode, but a classical competitive inhibition mode for PTP-MEG2 and SHP-2. The results demonstrate that both the structures of vanadium complexes and the conformations of PTPs influence PTP inhibition activity. Properly modifying the organic ligand moieties on vanadium may result in screening potent and selective vanadium-based PTP1B inhibitors.

Acknowledgements

This work was supported financially by the National Natural Science Foundation of China (20471033, 21001070 and 21171109), the Specialized Research Fund for the Doctoral Program of Higher Education (20111401110002), the Scientific Research Foundation for the Returned Overseas Chinese Scholars, State Education Ministry (20093602), the China Scholarship Council, the Natural Science Foundation of Shanxi Province (20051013, 2010011011-2, 2011011009-1 and 2011021006-2), Shanxi Scholarship Council of China (2012-004) and Instrumental Analysis Foundation of Large Scale Instruments of Shanxi University, China.

Notes and references

1 J. N. Andersen, P. G. Jansen, S. M. Echwald, O. H. Mortensen, T. Fukada, R. Del Vecchio, N. K. Tonks and N. P. Moller, *FASEB J.*, 2004, **18**, 8.
2 M. Stuible, K. M. Doody and M. L. Tremblay, *Cancer Metastasis Rev.*, 2008, **27**, 215.
3 K. M. Heinonen, F. P. Nestel, E. W. Newell, G. Charette, T. A. Seemayer, M. L. Tremblay and W. S. Lapp, *Blood*, 2004, **103**, 3457.
4 L. I. Pao, K. Badour, K. A. Siminovitch and B. G. Neel, *Annu. Rev. Immunol.*, 2007, **25**, 473.
5 T. Vang, A. V. Miletic, Y. Arimura, L. Tautz, R. C. Rickert and T. Mustelin, *Annu. Rev. Immunol.*, 2008, **26**, 29.
6 S. Hardy, S. G. Julien and M. L. Tremblay, *Anti-Cancer Agents Med. Chem.*, 2012, **12**, 4.
7 M. A. T. Blaskovich, *Curr. Med. Chem.*, 2009, **16**, 2095.
8 P. Heneberg, *Curr. Med. Chem.*, 2009, **16**, 706.
9 M. Elchebly, *Science*, 1999, **283**, 1544.
10 B. A. Zinker, C. M. Rondinone, J. M. Trevillyan, R. J. Gum, J. E. Clampit, J. F. Waring, N. Xie, D. Wilcox, P. Jacobson, L. Frost, P. E. Kroeger, R. M. Reilly, S. Koterski, T. J. Opgenorth, R. G. Ulrich, S. Crosby, M. Butler, S. F. Murray, R. A. McKay, S. Bhanot, B. P. Monia and M. R. Jirousek, *Proc. Natl. Acad. Sci. U. S. A.*, 2002, **99**, 11357.
11 R. Di Paola, L. Frittitta, G. Miscio, M. Bozzali, R. Baratta, M. Centra, D. Spampinato, M. G. Santagati, T. Ercolino, C. Cisternino, T. Soccio, S. Mastroianno, V. Tassi, P. Almgren, A. Pizzuti, R. Vigneri and V. Trischitta, *Am. J. Hum. Genet.*, 2002, **70**, 806.
12 T. Klupa, M. T. Malecki, M. Pezzolesi, L. Ji, S. Curtis, C. D. Langefeld, S. S. Rich, J. H. Warram and A. S. Krolewski, *Diabetes*, 2000, **49**, 2212.
13 N. D. Palmer, J. L. Bento, J. C. Mychaleckyj, C. D. Langefeld, J. K. Campbell, J. M. Norris, S. M. Haffner, R. N. Bergman and D. W. Bowden, *Diabetes*, 2004, **53**, 3013.
14 N. J. Spencer-Jones, X. L. Wang, H. Snieder, T. D. Spector, N. D. Carter and S. D. O'Dell, *Diabetes*, 2005, **54**, 3296.
15 S. Zhang and Z. Y. Zhang, *Drug Discovery Today*, 2007, **12**, 373.
16 A. J. Nichols, R. D. Mashal and B. Balkan, *Drug Dev. Res.*, 2006, **67**, 559.
17 K. H. Thompson and C. Orvig, *J. Inorg. Biochem.*, 2006, **100**, 1925.
18 H. Sakurai, Y. Yoshikawa and H. Yasui, *Chem. Soc. Rev.*, 2008, **37**, 2383.
19 D. A. Barrio and S. B. Etcheverry, *Curr. Med. Chem.*, 2010, **17**, 3632.
20 G. R. Willsky, L.-H. Chi, M. Godzala III, P. J. Kostyniak, J. J. Smee, A. M. Trujillo, J. A. Alfano, W. Ding, Z. Hu and D. C. Crans, *Coord. Chem. Rev.*, 2011, **255**, 2258.
21 J. H. McNeill, V. G. Yuen, S. Dai and C. Orvig, *Mol. Cell. Biochem.*, 1995, **153**, 175.
22 K. H. Thompson, J. Lichter, C. LeBel, M. C. Scaife, J. H. McNeill and C. Orvig, *J. Inorg. Biochem.*, 2009, **103**, 554.
23 D. C. Crans, J. J. Smee, E. Gaidamauskas and L. Q. Yang, *Chem. Rev.*, 2004, **104**, 849.
24 K. G. Peters, M. G. Davis, B. W. Howard, M. Pokross, V. Rastogi, C. Diven, K. D. Greis, E. Eby-Wilkens, M. Maier, A. Evdokimov, S. Soper and F. Genbauffe, *J. Inorg. Biochem.*, 2003, **96**, 321.
25 B. I. Posner, R. Faure, J. W. Burgess, A. P. Bevan, D. Lachance, G. Zhang-Sun, I. G. Fantus, J. B. Ng, D. A. Hall and B. S. Lum, *J. Biol. Chem.*, 1994, **269**, 4596.
26 G. Huyer, S. Liu, J. Kelly, J. Moffat, P. Payette, B. Kennedy, G. Tsaprailis, M. J. Gresser and C. Ramachandran, *J. Biol. Chem.*, 1997, **272**, 843.
27 F. Nxumalo, N. R. Glover and A. S. Tracey, *J. Biol. Inorg. Chem.*, 1998, **3**, 534.

28 C. Yuan, L. Lu, X. Gao, Y. Wu, M. Guo, Y. Li, X. Fu and M. Zhu, *J. Biol. Inorg. Chem.*, 2009, **14**, 841.
29 X. Gao, L. Lu, M. Zhu, C. Yuan, J. Ma and X. Fu, *Acta Chim. Sin.*, 2009, **67**, 929.
30 C. Yuan, L. Lu, Y. Wu, Z. Liu, M. Guo, S. Xing, X. Fu and M. Zhu, *J. Inorg. Biochem.*, 2010, **104**, 978.
31 L. Lu, S. Wang, M. Zhu, Z. Liu, M. Guo, S. Xing and X. Fu, *BioMetals*, 2010, **23**, 1139.
32 L. Lu and M. Zhu, *Anti-Cancer Agents Med. Chem.*, 2011, **11**, 164.
33 M. R. Karver, D. Krishnamurthy, R. A. Kulkarni, N. Bottini and A. M. Barrios, *J. Med. Chem.*, 2009, **52**, 6912.
34 C. Yuan, M. Zhu, Q. Wang, L. Lu, S. Xing, X. Fu, Z. Jiang, S. Zhang, Z. Li, Z. Li, R. Zhu, L. Ma and L. Xu, *Chem. Commun.*, 2012, **48**, 1153.
35 M. J. Clague, N. L. Keder and A. Butler, *Inorg. Chem*, 1993, **32**, 4754.
36 G.M. Sheldrick, *SADABS*, University of Göttingen, Germany, 2000.
37 G. M. Sheldrick, *Acta Crystallogr., Sect. A: Fundam. Crystallogr.*, 2008, **A64**, 112.
38 L. J. Farrugia, *J. Appl. Crystallogr.*, 1997, **30**, 565.
39 P. Gans, A. Sabatini and A. Vacca, *J. Chem. Soc., Dalton Trans.*, 1985, 1195.
40 E. M. Woolley, J. Tomkins and L. G. Hepler, *J. Solution Chem.*, 1972, **1**, 341.
41 B. Gyurcsik, T. Jakusch and T. Kiss, *J. Chem. Soc., Dalton Trans.*, 2001, 1053.
42 E. Lodyga-Chruscinska, D. Sanna, E. Garribba and G. Micera, *Dalton Trans*, 2008, 4903.
43 L. Ma, L. Lu, M. Zhu, Q. Wang, Y. Li, S. Xing, X. Fu, Z. Gao and Y. Dong, *Dalton Trans*, 2011, **40**, 6532.
44 Z. Zhu, M. Sun, X. Zhang, K. Liu, D. Shi, J. Li, J. Su, Y. Xu and X. Fu, *Chem. Res. Chin. Univ.*, 2007, **23**, 289.
45 Y. Qi, R. Zhao, H. Cao, X. Sui, S. B. Krantz and Z. Zhao, *J. Cell. Biochem.*, 2002, **86**, 79.
46 W. Li, Y. Zhuang, H. Li, Y. Sun, Y. Fu, X. Wu, Z. Zhao and X. Fu, *Chem. Res. Chin. Univ.*, 2008, **24**, 592.
47 S. Hati and D. Datta, *J. Chem. Soc., Dalton Trans.*, 1995, 1177.
48 I. N. Stepanenko, A. A. Krokhin, R. O. John, A. Roller, V. B. Arion, M. A. Jakupec and B. K. Keppler, *Inorg. Chem.*, 2008, **47**, 7338.
49 M. Li, W. Ding, B. Baruah, D. C. Crans and R. Wang, *J. Inorg. Biochem.*, 2008, **102**, 1846.